Journal of Theoretical and Applied Vibration and Acoustics 7(2) 99-117 (2021)

I S A V

Journal of Theoretical and Applied

Vibration and Acoustics

journal homepage: http://tava.isav.ir

Robust adaptive vibration control of nonlocal strain gradient

Mohammad Reza Hairi Yazdi*[a], Amin Vahidi-Moghaddam[b], Amin Yousefpour[c]

[a] *Professor, Department of Mechanical Engineering, University of Tehran, Tehran, Iran*

[b] *Ph.D. Student, Department of Mechanical Engineering, Michigan State University, East Lansing, USA*

[c] *MSc Student, Department of Mechanical Engineering, University of Tehran, Tehran, Iran*

ARTICLE INFO

Article history:
Received 25 February 2021

Received in revised form
5 June 2021

Accepted 23 October 2021

Available online 15 December 2021

Keywords:
Nonlocal strain gradient theory,

Hamiltonian principle,

Nonlinear forced vibrations,

Extended Kalman filter,

ABSTRACT

An Euler–Bernoulli nanobeam is stabilized using a robust adaptive sliding mode control. Using nonlocal strain gradient theory and Hamilton's principle, a nonlinear partial differential equation is derived to demonstrate the vibration behavior of the considered nanobeam. Moreover, the obtained partial differential equation is converted to an ordinary differential equation using the Galerkin technique. To suppress the nonlinear vibration of the nanobeam and overcome the uncertainties, robust adaptive vibration control is designed using an extended Kalman filter and sliding mode control. Finally, simulation results show the performance of the designed robust adaptive controller. Furthermore, the traditional control schemes are used to illustrate the superiority of the proposed controller over them.

1. Introduction

Micro/nano-beams have many applications in micro/nano-electromechanical systems, including bio-MEMS [1], atomic force microscopes [2], micro-switches [3], micro-actuators [4], micro-resonators [5], and carbon nanotubes [6]. For instance, micro/nanobeams are used in micro/nano-

* Corresponding author:
E-mail addres: myazdi@ut.ac.ir (M.R. Hairi Yazdi)

http://dx.doi.org/10.22064/tava.2022.532276.1184

mirror tilts to control the tilt of mirrors [7] and also in printers to increase the speed of printing with better quality [8]. Theoretical studies and experimental observations, such as atomistic analysis methods and continuum mechanics theory, are used to investigate the mechanical behaviors of micro/nanobeams. However, the atomistic methods take a lot of time for analysis, and the classical continuum theory is inaccurate for micro/nano-structures since it does not consider the additional length scale parameters. Consequently, the non-classical continuum theory is commonly used in micro/nano-scale analysis since it is accurate and does not require a long time analysis [9].

To capture the size-dependent behaviors of the micro/nanobeams, the couple stress theory has been introduced as one of the non-classical continuum theories [10, 11]. Also, the strain gradient theory has been proposed such that the strain energy is a function of its first derivative and the amount of strain [12-14]. Moreover, the nonlocal elasticity theory illustrates that the strains at all points in the continuum play important roles in the stress at a point [15]. However, the nonlocal elasticity theory does not consider the effect of stiffness enhancement and characterizes only the softening effect; thus, the strain gradient theory can be used to handle this issue. Consequently, to precisely capture the size-dependent behaviors of the micro/nanobeams, a combination of the nonlocal elasticity theory [15] and the strain gradient theory [16] has been proposed as the nonlocal strain gradient theory [17].

Large transverse loads cause a nonlinear vibration behavior for the micro/nanobeams with axially immovable ends since an axial tension is generated; however, the immovable ends keep the strains small. Recently, many researchers have studied the nonlinear static and vibration behavior of the micro/nanobeams [5, 18, 19]. To prevent the micro/nanobeams from damage, one can use vibration control strategies, which can improve the performance and resolution of the system. However, the micro/nanobeam models usually include model uncertainties due to imperfect measurement; therefore, robust adaptive control schemes are useful to enhance accuracy. The popular approaches for estimation and stabilization are respectively the extended Kalman filter (EKF) algorithm [20-22] and the sliding mode control (SMC) [23-26] which help us reduce the tracking error for the nonlinear systems with model uncertainty. Ayati et al. [27] employed the EKF algorithm to estimate the state and parameters of a nonlinear chaotic system. Moreover, the EKF has been employed to estimate the state of the non-classical microcantilevers by Vatankhah et al. [28].

In this work, a robust adaptive vibration control strategy is developed to suppress the nonlinear vibrations of nanobeams. The Galerkin technique is utilized to convert the governing nonlinear partial differential equation to the nonlinear ordinary differential equation with cubic nonlinearity. The SMC is used to stabilize the nonlinear vibrations of the nanobeams, and the stability of the closed-loop system is proved using the Lyapunov stability theorem. Moreover, the EKF is employed to estimate the states of the system using the noisy output. Finally, simulation results are shown to verify the performance of the developed controller for stabilizing the nonlinear vibrations of nanobeams.

The paper is organized as follows. In Section 2, a mathematical model is presented for an Euler-Bernoulli nonlocal strain gradient nanobeam under a centralized force in the middle of the beam. Section 3 outlines the design of SMC and the EKF algorithm is presented for uncertain nanobeams. Section 4 provides numerical simulations that prove the proposed control scheme is successful in stabilizing the nonlinear vibration of nanobeam. The conclusions are drawn in Section 5.

2. System model and mathematical formulation

For an isotropic linear elastic material, the strain energy (U) is considered using the nonlocal strain gradient theory via the following correlation [17]:

$$U = \frac{1}{2}\int_V (\sigma_{xx}\,\varepsilon_{xx} + \sigma_{xx}^{(1)}\,\nabla\varepsilon_{xx})dV \tag{1}$$

where ε_{xx}, σ_{xx}, and $\sigma_{xx}^{(1)}$ indicate the normal strain, the classical stress, and the higher-order stress, respectively. Also, the one-dimensional differential operator is represented by ∇ which is $\partial/\partial x$. The components of σ_{xx} and $\sigma_{xx}^{(1)}$ are expressed as follows.

$$\sigma_{xx} = \int_0^L E\,\alpha_0(x,x',e_0a)\,\varepsilon'_{xx}(x')dx' \tag{2}$$

$$\sigma_{xx}^{(1)} = l_m{}^2\int_0^L E\,\alpha_1(x,x',e_1a)\,\varepsilon'_{xx,x}(x')dx' \tag{3}$$

$$t_{xx} = \sigma_{xx} - \nabla\sigma_{xx}^{(1)} \tag{4}$$

where E, α_0, α_1, and L respectively stand for Young's modulus, the nonlocal effects, and the length of the nanobeam. In addition, the effects of the nonlocal elastic stress field are expressed by e_0a and e_1a. Moreover, the effect of strain gradient is represented by l_m. Consequently, the general nonlocal strain gradient constitutive equation is obtained as [17]

$$\left[1-(e_0a)^2\nabla^2\right]\left[1-(e_1a)^2\nabla^2\right]t_{xx} = E\left[1-(e_1a)^2\nabla^2\right]\varepsilon_{xx} - E\,l_m{}^2\left[1-(e_0a)^2\nabla^2\right]\nabla^2\varepsilon_{xx} \tag{5}$$

where $\nabla^2 = \partial^2/\partial x^2$ is the Laplacian operator. If $e_0 = e_1 = e$, Eq. (5) is rewritten as:

$$\left[1-(ea)^2\nabla^2\right]t_{xx} = E\,(1-l_m{}^2\nabla^2)\varepsilon_{xx} \tag{6}$$

Supposing $l_m = 0$ results in nonlocal elasticity theory as [15]

$$\left[1-(ea)^2\nabla^2\right]t_{xx} = E\,\varepsilon_{xx} \tag{7}$$

Also, considering $ea = 0$ results in strain gradient theory as [16]

$$t_{xx} = E\,(1-l_m{}^2\nabla^2)\varepsilon_{xx} \tag{8}$$

The structure of a hinged–hinged Euler–Bernoulli nanobeams is illustrated in Figure 1, and the displacement components are given as

$$\begin{aligned} u_1(x,z,t) &= u(x,t) - z\,\frac{\partial w(x,t)}{\partial x} \\ u_2(x,z,t) &= 0 \\ u_3(x,z,t) &= w(x,t) \end{aligned} \tag{9}$$

where the displacements along the x, y, and z axes are represented by u_x, u_y , and u_Z, respectively. w and u are the transverse and axial deflections, t and x denote the independent time and spatial variables, and $\partial w/\partial x$ represents the angle of rotation of the beam cross-section (about the y-axis). The Von-Karman's nonlinear strain relationship is obtained by assuming a large deflection and small slope for a straight Euler–Bernoulli nanobeam as follows

$$\varepsilon_{xx} = \frac{\partial u(x,t)}{\partial x} + \frac{1}{2}\left(\frac{\partial w(x,t)}{\partial x}\right)^2 - z\,\frac{\partial^2 w(x,t)}{\partial x^2} \tag{10}$$

where ε_{xx} denotes the longitudinal strain. The first variation of strain energy is given by

$$\delta\int_0^t U\,dt = \int_0^t\int_V (\sigma_{xx}\,\delta\varepsilon_{xx} + \sigma_{xx}^{(1)}\nabla\delta\varepsilon_{xx})\,dV\,dt \tag{11}$$

where Eq. (11) can be rewritten as follows

$$\begin{aligned} \delta\int_0^t U\,dt &= \int_0^t\int_V (\sigma_{xx}\,\delta\varepsilon_{xx} - \nabla\sigma_{xx}^{(1)}\,\delta\varepsilon_{xx})\,dV\,dt + \int_0^t \left[\int_A \sigma_{xx}^{(1)}\,\delta\varepsilon_{xx}\,dA\right]_0^L dt \\ &= \int_0^t\int_V (t_{xx}\,\delta\varepsilon_{xx})\,dV\,dt + \int_0^t \left[\int_A \sigma_{xx}^{(1)}\,\delta\varepsilon_{xx}\,dA\right]_0^L dt \end{aligned} \tag{12}$$

where A is the cross-sectional area. The following resultant stress is defined as:

$$N_c = \int_A t_{xx}\,dA,\; M_c = \int_A z\,t_{xx}\,dA,\; N_{nc} = \int_A \sigma_{xx}^{(1)}\,dA,\; M_{nc} = \int_A z\,\sigma_{xx}^{(1)}\,dA \tag{13}$$

where $\boldsymbol{M_c}$ and $\boldsymbol{N_c}$ are respectively the classical normal moment and force. Also, $\boldsymbol{M_{nc}}$ and $\boldsymbol{N_{nc}}$ indicate the non-classical ones. Substituting Eqs. (10) and (13) into Eq. (12) results in

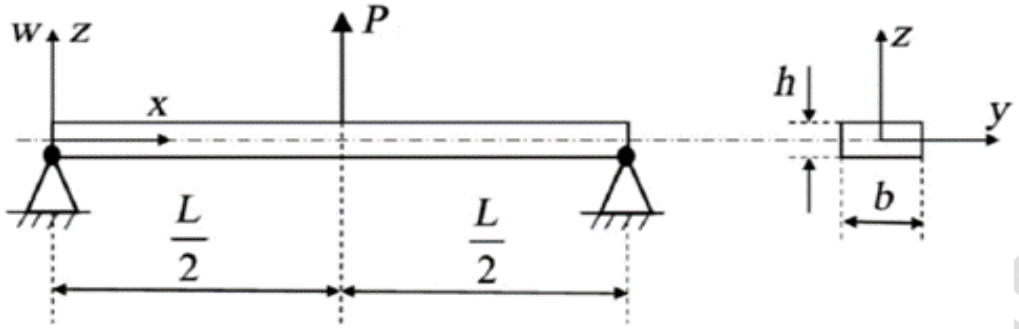

Fig. (1) A hinged-hinged nanobeam.

$$\delta\int_0^t U\,dt=\int_0^t\int_0^L\left[N_c\left(\frac{\partial\delta u}{\partial x}+\frac{\partial w}{\partial x}\frac{\partial\delta w}{\partial x}\right)-M_c\frac{\partial^2\delta w}{\partial x^2}\right]dx\,dt \\ +\int_0^t\left[N_{nc}\left(\frac{\partial\delta u}{\partial x}+\frac{\partial w}{\partial x}\frac{\partial\delta w}{\partial x}\right)-M_{nc}\frac{\partial^2\delta w}{\partial x^2}\right]_0^L dt \tag{14}$$

Also, for the work, which is generated by the applied external forces, one has

$$\delta\int_0^t W\,dt=\int_0^t\int_L(f\,\delta u+q\,\delta w)dx\,dt \tag{15}$$

where f and q are the distributed axial and transverse loads.

Now, the first variation of kinetic energy is given as

$$\delta\int_0^t K_e\,dt=\int_0^t\int_0^L I_A\left(\frac{\partial u}{\partial t}\frac{\partial\delta u}{\partial t}+\frac{\partial w}{\partial t}\frac{\partial\delta w}{\partial t}\right)dx\,dt \tag{16}$$

where,

$$I_A=\frac{1}{12}bh^3 \tag{17}$$

Now, the general form of Hamilton's principle is given by

$$\delta\int_0^t\left[K_e-(U-W)\right]dt=0 \tag{18}$$

Using Eq. (18) and separating the coefficients of δu and δw, the governing equation of the system is obtained as follows

$$\delta u \Rightarrow \frac{\partial N_c}{\partial x} + f(x,t) = I_A \frac{\partial^2 u}{\partial t^2}$$
$$\delta w \Rightarrow \frac{\partial^2 M_c}{\partial x^2} + \frac{\partial}{\partial x}(N_c \frac{\partial w}{\partial x}) + q(x,t) = I_A \frac{\partial^2 w}{\partial t^2} \quad (19)$$

where the corresponding boundary conditions are

$$\delta u \Rightarrow N_c = 0 \text{ or } u = 0$$
$$\frac{\delta \partial u}{\partial x} \Rightarrow N_{nc} = 0 \text{ or } \frac{\partial u}{\partial x} = 0$$
$$\delta w \Rightarrow \frac{\partial M_c}{\partial x} + N_c \frac{\partial w}{\partial x} = 0 \text{ or } w = 0 \quad (20)$$
$$\frac{\delta \partial w}{\partial x} \Rightarrow M_c - N_{nc} \frac{\partial w}{\partial x} = 0 \text{ or } \frac{\partial w}{\partial x} = 0$$
$$\frac{\delta \partial^2 w}{\partial x^2} \Rightarrow M_{nc} = 0 \text{ or } \frac{\partial^2 w}{\partial x^2} = 0$$

Now, Eq. (6) is developed for the nanobeam using the nonlocal strain gradient theory as follows

$$t_{xx} - (e\,a)^2 \frac{\partial^2 t_{xx}}{\partial x^2} = E\left[\frac{\partial u}{\partial x} + \frac{1}{2}(\frac{\partial w}{\partial x})^2 - z\frac{\partial^2 w}{\partial x^2}\right] - E\,l_m^2\left[\frac{\partial^3 u}{\partial x^3} + \frac{\partial w}{\partial x}\frac{\partial^3 w}{\partial x^3} + (\frac{\partial^2 w}{\partial x^2})^2 - z\frac{\partial^4 w}{\partial x^4}\right] \quad (21)$$

According to Eqs. (13) and (21), one has

$$N_c - (e\,a)^2 \frac{\partial^2 N_c}{\partial x^2} = A_{xx}\left[\frac{\partial u}{\partial x} + \frac{1}{2}(\frac{\partial w}{\partial x})^2\right] - A_{xx}\,l_m^2\left[\frac{\partial^3 u}{\partial x^3} + \frac{\partial w}{\partial x}\frac{\partial^3 w}{\partial x^3} + (\frac{\partial^2 w}{\partial x^2})^2\right] \quad (22)$$
$$M_c - (e\,a)^2 \frac{\partial^2 M_c}{\partial x^2} = -D_{xx}\frac{\partial^2 w}{\partial x^2} + D_{xx}\,l_m^2 \frac{\partial^4 w}{\partial x^4}$$

Where

$$(A_{xx}, D_{xx}) = \int_A E\,(1, z^2)\,dA, \quad B_{xx} = \int_A E\,z\,dA = 0 \quad (23)$$

Now, using Eq. (19), substituting $\frac{\partial N_c}{\partial x}$ and $\frac{\partial^2 M_c}{\partial x^2}$ into Eq. (22) yields

$$N_c = A_{xx}\left[\frac{\partial u}{\partial x} + \frac{1}{2}(\frac{\partial w}{\partial x})^2\right] - A_{xx}\,l_m^2\left[\frac{\partial^3 u}{\partial x^3} + \frac{\partial w}{\partial x}\frac{\partial^3 w}{\partial x^3} + (\frac{\partial^2 w}{\partial x^2})^2\right] + (e\,a)^2(I_A\frac{\partial^3 u}{\partial t^2 \partial x} - \frac{\partial f}{\partial x})$$
$$M_c = -D_{xx}\frac{\partial^2 w}{\partial x^2} + D_{xx}\,l_m^2\frac{\partial^4 w}{\partial x^4} + (e\,a)^2\left[I_A\frac{\partial^2 w}{\partial t^2} - \frac{\partial}{\partial x}(N_c\frac{\partial w}{\partial x}) - q\right] \quad (24)$$

Moreover, substituting Eq.(19) in Eq.(24) yields

$$\begin{aligned}
&\frac{\partial}{\partial x}\left\{\left[A_{xx}\frac{\partial u}{\partial x}+\frac{A_{xx}}{2}(\frac{\partial w}{\partial x})^2\right]-\left[A_{xx}\,l_m{}^2\frac{\partial^3 u}{\partial x^3}+A_{xx}\,l_m{}^2(\frac{\partial w}{\partial x}\frac{\partial^3 w}{\partial x^3}+(\frac{\partial^2 w}{\partial x^2})^2)\right]\right\}\\
&+I_A\frac{\partial^2}{\partial t^2}\left[(e\,a)^2\frac{\partial^2 u}{\partial x^2}-u\right]=(e\,a)^2\frac{\partial^2 f}{\partial x^2}-f\\
&D_{xx}\,l_m{}^2\frac{\partial^6 w}{\partial x^6}-D_{xx}\frac{\partial^4 w}{\partial x^4}+\frac{\partial}{\partial x}(N_c\frac{\partial w}{\partial x})-(e\,a)^2\frac{\partial^3}{\partial x^3}(N_c\frac{\partial w}{\partial x})\\
&+I_A\frac{\partial^2}{\partial t^2}\left[(e\,a)^2\frac{\partial^2 w}{\partial x^2}-w\right]=(e\,a)^2\frac{\partial^2 q}{\partial x^2}-q
\end{aligned}\tag{25}$$

Considering the negligible rotational inertia of the beam, the governing equation, which is a function of u and its derivatives, is expressed as

$$\frac{\partial}{\partial x}\left\{\left[A_{xx}\frac{\partial u}{\partial x}+\frac{A_{xx}}{2}(\frac{\partial w}{\partial x})^2\right]-\left[A_{xx}\,l_m{}^2\frac{\partial^3 u}{\partial x^3}+A_{xx}\,l_m{}^2(\frac{\partial w}{\partial x}\frac{\partial^3 w}{\partial x^3}+(\frac{\partial^2 w}{\partial x^2})^2)\right]\right\}=\frac{\partial}{\partial x}(N_c)=0 \tag{26}$$

According to Eq. (26), it can be concluded that N_c remains unchanged. Integrating both sides of Eq. (26), the following equation is derived.

$$\frac{\partial u}{\partial x}+\frac{1}{2}(\frac{\partial w}{\partial x})^2-l_m{}^2\frac{\partial^3 u}{\partial x^3}-l_m{}^2(\frac{\partial w}{\partial x}\frac{\partial^3 w}{\partial x^3}+(\frac{\partial^2 w}{\partial x^2})^2)=\frac{C}{A_{xx}} \tag{27}$$

where C is a constant parameter. The boundary condition for the hinged-hinged beam is defined as

$$u(0,t)=u(L,t)=\frac{\partial^2 u(0,t)}{\partial x^2}=\frac{\partial^2 u(L,t)}{\partial x^2}=0 \tag{28}$$

According to Eq. (28), the strain gradient theory [16] and the boundary conditions, one can reach the following equation by integrating both sides of (27) over the beam length ($x = 0\ to\ x = L$).

$$\begin{aligned}
\frac{C\,L}{A_{xx}}&=\left[u(L,t)-u(0,t)\right]-l_m{}^2\left[\frac{\partial^2 u(L,t)}{\partial x^2}-\frac{\partial^2 u(0,t)}{\partial x^2}\right]\\
&+\frac{1}{2}\int_0^L(\frac{\partial w}{\partial x})^2dx-l_m{}^2\int_0^L(\frac{\partial w}{\partial x}\frac{\partial^3 w}{\partial x^3}+(\frac{\partial^2 w}{\partial x^2})^2)dx
\end{aligned}\tag{29}$$

Hence

$$\frac{C\,L}{A_{xx}}=\left[u(L,t)-u(0,t)\right]-l_m{}^2\left[\frac{\partial^2 u(L,t)}{\partial x^2}-\frac{\partial^2 u(0,t)}{\partial x^2}\right]+\frac{1}{2}\int_0^L(\frac{\partial w}{\partial x})^2\,dx-l_m{}^2\int_0^L(\frac{\partial w}{\partial x}\frac{\partial^3 w}{\partial x^3}+(\frac{\partial^2 w}{\partial x^2})^2)dx \tag{30}$$

$$N_c=\frac{A_{xx}}{2L}\int_0^L(\frac{\partial w}{\partial x})^2\,dx-\frac{A_{xx}\,l_m{}^2}{L}\int_0^L(\frac{\partial w}{\partial x}\frac{\partial^3 w}{\partial x^3}+(\frac{\partial^2 w}{\partial x^2})^2)dx \tag{31}$$

Now, substituting Eq. (31) into Eq. (25) yields the governing equation of the nonlocal strain gradient nanobeam as follows [9]

$$D_{xx}\,l_m{}^2\frac{\partial^6 w}{\partial x^6}-D_{xx}\frac{\partial^4 w}{\partial x^4}+\left[\frac{A_{xx}}{2L}\int_0^L(\frac{\partial w}{\partial x})^2\,dx-\frac{A_{xx}\,l_m{}^2}{L}\int_0^L(\frac{\partial w}{\partial x}\frac{\partial^3 w}{\partial x^3}+(\frac{\partial^2 w}{\partial x^2})^2)dx\right]\times\left[\frac{\partial^2 w}{\partial x^2}-(e\,a)^2\frac{\partial^4 w}{\partial x^4}\right]+I_A\frac{\partial^2}{\partial t^2}\left[(e\,a)^2\frac{\partial^2 w}{\partial x^2}-w\right]=(e\,a)^2\frac{\partial^2 q}{\partial x^2}-q \tag{32}$$

The following non-dimensional quantities are introduced in order to develop the dimensionless form of the equation (32)

$$\bar{x}=\frac{x}{L},\ \bar{w}=\frac{w}{r},\ \bar{z}=\frac{z}{h},\ \bar{t}=t\sqrt{\frac{E\,I}{\rho A L^4}},\ \alpha=\frac{e\,a}{L},\ \beta=\frac{l_m}{L} \tag{33}$$

where $r=\sqrt{I/A}$. Therefore, the dimensionless governing equation is obtained as follows

$$\beta^2\bar{D}_{xx}\frac{\partial^6\bar{w}}{\partial\bar{x}^6}-\bar{D}_{xx}\frac{\partial^4\bar{w}}{\partial\bar{x}^4}+\left[\frac{\bar{A}_{xx}}{2}\int_0^1(\frac{\partial\bar{w}}{\partial\bar{x}})^2\,d\bar{x}-\beta^2\bar{A}_{xx}\int_0^1(\frac{\partial\bar{w}}{\partial\bar{x}}\frac{\partial^3\bar{w}}{\partial\bar{x}^3}+(\frac{\partial^2\bar{w}}{\partial\bar{x}^2})^2)d\bar{x}\right]\frac{\partial^2\bar{w}}{\partial\bar{x}^2}-\left[\frac{\alpha^2\bar{A}_{xx}}{2}\int_0^1(\frac{\partial\bar{w}}{\partial\bar{x}})^2\,d\bar{x}-\alpha^2\beta^2\bar{A}_{xx}\int_0^1(\frac{\partial\bar{w}}{\partial\bar{x}}\frac{\partial^3\bar{w}}{\partial\bar{x}^3}+(\frac{\partial^2\bar{w}}{\partial\bar{x}^2})^2)d\bar{x}\right]\frac{\partial^4\bar{w}}{\partial\bar{x}^4}+\alpha^2\bar{I}_A\frac{\partial^4\bar{w}}{\partial\bar{x}^2\partial\bar{t}^2}-\bar{I}_A\frac{\partial^2\bar{w}}{\partial\bar{t}^2}=\alpha^2\frac{\partial^2\bar{q}}{\partial\bar{x}^2}-\bar{q} \tag{34}$$

Where

$$\bar{A}_{xx}=1,\ \bar{D}_{xx}=1,\ \bar{I}_A=1 \tag{35}$$

Herein, through the Galerkin approach, the obtained partial differential equation is converted to the nonlinear ordinary differential equation. To this end, we decompose the temporal and spatial terms of $\bar{w}(\bar{x},\bar{t})$ as follows [29]

$$\bar{w}(\bar{x},\bar{t})=Q(\bar{t})\,\phi(\bar{x}) \qquad \phi(\bar{x})=\sin(\pi\bar{x}) \tag{36}$$

where $Q(\bar{t})$ stands for the unknown temporal part of the transverse deflection, and $\phi(\bar{x})$ indicates the spatial part and satisfies the boundary conditions of the hinged-hinged nanobeam. Also, the concentrated force $\bar{q}(\bar{x},\bar{t})$ is given by

$$\bar{q}(\bar{x},\bar{t})=q(\bar{t})\,\delta(\bar{x}-\frac{1}{2})$$
$$\int_{a-\varepsilon}^{a+\varepsilon} f(x)\,\delta(x-a)dx=f(a),\quad \int_{a-\varepsilon}^{a+\varepsilon} f(x)\,\delta^{(n)}(x-a)dx=-\int_{a-\varepsilon}^{a+\varepsilon}\frac{\partial f}{\partial x}\,\delta^{(n-1)}(x-a)dx \tag{37}$$

Substituting Eqs. (36) and (37) in Eq. (34), multiplying both sides of Eq. (34) by $\phi(\bar{x})$, and integrating over the beam length, the ODE will be obtained as follows

$$\ddot{Q}(\bar{t})+K_1 Q(\bar{t})+K_2 Q^3(\bar{t})=-(\alpha^2\pi^2+1)\,q(\bar{t}) \tag{38}$$

where the coefficients K_1 and K_2 are given by

$$K_1=\frac{\beta^2\bar{D}_{xx}\int_0^1\phi^{(6)}\phi\,d\bar{x}-\bar{D}_{xx}\int_0^1\phi^{(4)}\phi\,d\bar{x}}{\alpha^2\int_0^1\phi''\phi\,d\bar{x}-\int_0^1(\phi)^2\,d\bar{x}} \tag{39}$$

$$K_2=-\frac{\frac{\bar{A}_{xx}}{2}\int_0^1(\phi')^2d\bar{x}.\int_0^1\phi''\phi d\bar{x}-\beta^2\bar{A}_{xx}\int_0^1\phi'''\phi'd\bar{x}.\int_0^1\phi''\phi d\bar{x}-\beta^2\bar{A}_{xx}\int_0^1(\phi'')^2d\bar{x}.\int_0^1\phi''\phi d\bar{x}}{\alpha^2\int_0^1\phi''\phi d\bar{x}-\int_0^1(\phi)^2d\bar{x}}$$
$$-\frac{\frac{\alpha^2\bar{A}_{xx}}{2}\int_0^1(\phi')^2d\bar{x}.\int_0^1\phi^{(4)}\phi d\bar{x}-\alpha^2\beta^2\bar{A}_{xx}\int_0^1\phi'''\phi'd\bar{x}.\int_0^1\phi^{(4)}\phi d\bar{x}-\alpha^2\beta^2\bar{A}_{xx}\int_0^1(\phi'')^2d\bar{x}.\int_0^1\phi^{(4)}\phi d\bar{x}}{\alpha^2\int_0^1\phi''\phi d\bar{x}-\int_0^1(\phi)^2d\bar{x}} \tag{40}$$

where $\phi^{(4)}$ and $\phi^{(6)}$ are respectively fourth and sixth derivatives of ϕ with respect to time, and ϕ' is its first derivative with respect to $\bar{x}$.

3. Control design

Herein, we propose a robust adaptive SMC to suppress the nonlinear forced vibration of the hinged–hinged nanobeam. Evidently, in micro/nano-systems, the existence of uncertainties is

undeniable. Hence, implementing a robust controller for such systems is of crucial necessity. To design a robust controller, we consider the following uncertain parameters for the system as follows

$$\begin{aligned} K_{1\min} < K_1 < K_{1\max} \\ K_{2\min} < K_2 < K_{2\max} \\ b_{\min} < b < b_{\max} \end{aligned} \tag{41}$$

The state-space equation of the system is

$$\begin{aligned} & Q(\bar{t}) = x_1, \dot{Q}(\bar{t}) = \dot{x}_1 = x_2 \\ & \begin{cases} \dot{x}_1 = x_2 \\ \dot{x}_2 = -K_1 x_1 - K_2 (x_1)^3 - b\, q(\bar{t}) \end{cases} \end{aligned} \tag{42}$$

3.1. Robust adaptive SMC

Now, we design a second-order sliding surface as

$$S = (\frac{d}{dt} + \lambda)^{n-1} e \tag{43}$$

where $\lambda > 0$, and $(\frac{d}{dt} + \lambda)^{n-1} e$ is a Routh-Hurwitz equation of error e, which satisfies the stability of the system when it is on the sliding surface.

For the uncertain nonlinear system (42), the robust SMC is designed as

$$u = u_{eq} + v \tag{44}$$

where u_{eq} is obtained for $\dot{s} = 0$ and is equal to

$$\begin{aligned} & \dot{s} = \lambda x_2 - K_1 x_1 - K_2 x_1^3 - b u_{eq} = 0 \\ & \Rightarrow u_{eq} = \frac{\lambda x_2 - \hat{K}_1 x_1 - \hat{K}_2 x_1^3}{\hat{b}} \end{aligned} \tag{45}$$

and v is obtained for $s\dot{s} \le -\eta s$ and $\eta > 0$ as

$$\begin{aligned} & \dot{V} = s\dot{s} = s(\lambda x_2 - K_1 x_1 - K_2 x_1^3 - bu) \le -\eta |s| \\ & \Rightarrow s\lambda(1 - \frac{b}{\hat{b}}) x_2 + s(\frac{b}{\hat{b}} \hat{K}_1 - K_1) x_1 + s(\frac{b}{\hat{b}} \hat{K}_2 - K_2) x_1^3 - s\, b\, v \\ & \le |s| \lambda(1 - \frac{b_{\min}}{\hat{b}}) |x_2| + |s| (\frac{b_{\max}}{\hat{b}} \hat{K}_1 - K_{1\min}) |x_1| + |s| (\frac{b_{\max}}{\hat{b}} \hat{K}_2 - K_{2\min}) |x_1^3| - s\, b_{\min} v \le -\eta |s| \end{aligned} \tag{46}$$

Thus, for $K \ge \eta$, one has

$$v=\frac{1}{b_{\min}}\left(\lambda(1-\frac{b_{\min}}{\hat{b}})\left|x_2\right|+(\frac{b_{\max}}{\hat{b}}\hat{K}_1-K_{1\min})\left|x_1\right|+(\frac{b_{\max}}{\hat{b}}\hat{K}_2-K_{2\min})\left|x_1^3\right|+K\right)sign(S) \quad (47)$$

The designed control approach suffers from the chattering caused by the discontinuous function $sign(.)$; thus, the following $Sat(.)$ function is used to handle this issue as

$$Sat(\frac{s}{\phi})=\begin{cases} sign(s) & |s|\geq\phi \\ \frac{s}{\phi} & |s|<\phi \end{cases} \quad (48)$$

where ϕ is the boundary layer thickness. Therefore, considering $\lambda=1$, the control law is

$$\begin{aligned} u&=u_{eq}+u_c \\ &=\frac{-x_2+\hat{K}_1 x_1+\hat{K}_2(x_1)^3}{\hat{b}} \\ &+\frac{1}{b_{\min}}\left((1-\frac{b_{\min}}{\hat{b}})\left|x_2\right|+(\frac{b_{\max}}{\hat{b}}\hat{K}_1-K_{1\min})\left|x_1\right|+(\frac{b_{\max}}{\hat{b}}\hat{K}_2-K_{2\min})\left|x_1^3\right|+K\right)Sat(\frac{s}{\phi}) \end{aligned} \quad (49)$$

3.2. Extended Kalman filter

Accurate information about the states of the system is necessary for designing a controller; however, we may not be able to measure the states in some applications. Hence, in the current study, the extended Kalman filter (EKF) is implemented to approximate the state of the system. The discrete form of the considered system is given as

$$\begin{aligned} &\dot{x}=\frac{x_{(k)}-x_{(k-1)}}{T_s} \\ &\begin{cases} x_{1(k)}=x_{1(k-1)}+T_s\,x_{2(k-1)}+w_{1(k-1)} \\ x_{2(k)}=x_{2(k-1)}+T_s(-K_1\,x_{1(k-1)}-K_2\,x^3{}_{1(k-1)}-b\,u_{(k-1)})+w_{2(k-1)} \end{cases} \\ &y_{(k-1)}=x_{1(k-1)}+v_{(k-1)} \end{aligned} \quad (50)$$

The measurement and process noises are considered as white noises with zero mean value, and covariance matrices R and Q are as follows

$$\begin{aligned} Q&=\begin{bmatrix} q^2 & 0 \\ 0 & q^2 \end{bmatrix} \\ R&=r^2 \end{aligned} \quad (51)$$

where $q=r=0.01$. The generalized discrete dynamic state model is expressed as

$$\begin{aligned} x_{(k)}&=f(x_{(k-1)})+w_{(k-1)} \\ y_{(k)}&=h(x_{(k-1)})+v_{(k-1)} \end{aligned} \quad (52)$$

where w and v respectively denote the process and measurement noise vectors, and the output of the system is represented by y. First, in the prediction process, a prediction of the covariance matrix and the states are obtained based on the previous states as

$$\begin{aligned} \hat{x}_{(k|k-1)} &= f\,(\hat{x}_{(k-1|k-1)}) \\ P_{(k|k-1)} &= F_{(k-1)}\,P_{(k-1|k-1)}\,F^{T}{}_{(k-1)} + Q_{(k-1)} \end{aligned} \tag{53}$$

where $\hat{x}_{(k|k-1)}$ denotes the estimated state at time k based on the previous data. Also, $P_{(k|k-1)}$ and f indicate the prediction error covariance matrix and the state transition function, respectively. Then, in the second step, the covariance matrix and predicted states would be corrected, and the following recursive relations present this process as

$$\begin{aligned} B_{(k)} &= y_{(k)} - h(\hat{x}_{(k|k-1)}) \\ S_{(k)} &= H_{(k)}\,P_{(k|k-1)}H^{T}{}_{(k)} + R_{(k)} \\ K_{(k)} &= P_{(k|k-1)}H^{T}{}_{(k)}\,S^{-1}{}_{(k)} \\ \hat{x}_{(k|k)} &= \hat{x}_{(k|k-1)} + K_{(k)}\,B_{(k)} \\ P_{(k|k)} &= P_{(k|k-1)} - K_{(k)}\,S_{(k)}\,K^{T}{}_{(k)} \end{aligned} \tag{54}$$

where $K, B,$ and S denote the estimation gains. Also, F and H are the Jacobian matrices of the system which can be obtained as follows

$$\begin{aligned} \left[F_{(k)}\right]_{i,j} &= \left.\frac{\partial f_i(x)}{\partial x_j}\right|_{x=\hat{x}_{(k|k)}} \\ \left[H_{(k)}\right]_{i,j} &= \left.\frac{\partial h_i(x)}{\partial x_j}\right|_{x=\hat{x}_{(k|k-1)}} \end{aligned} \tag{55}$$

4. Numerical Simulations

In this section, the numerical simulation for the stabilization of the nanobeam is demonstrated using the proposed robust adaptive sliding mode control. For numerical simulations, the parameters of the nonlocal strain gradient nanobeam are considered as $\alpha = \beta = 0.1$; consequently, the exact value of appeared parameters in (38) is obtained as $K_1 = 97.4$, $K_2 = -19.97$, and $b = 1.09$. To consider the model uncertainty for the nanobeam models, we consider the following uncertainty ranges for the parameters as

$$\begin{aligned} &\hat{K}_1 = 97.4,\ 90 < K_1 < 100 \\ &\hat{K}_2 = -19.97,\ -20 < K_2 < -19 \\ &\hat{b} = 1.09,\ 1 < b < 1.1 \end{aligned} \tag{56}$$

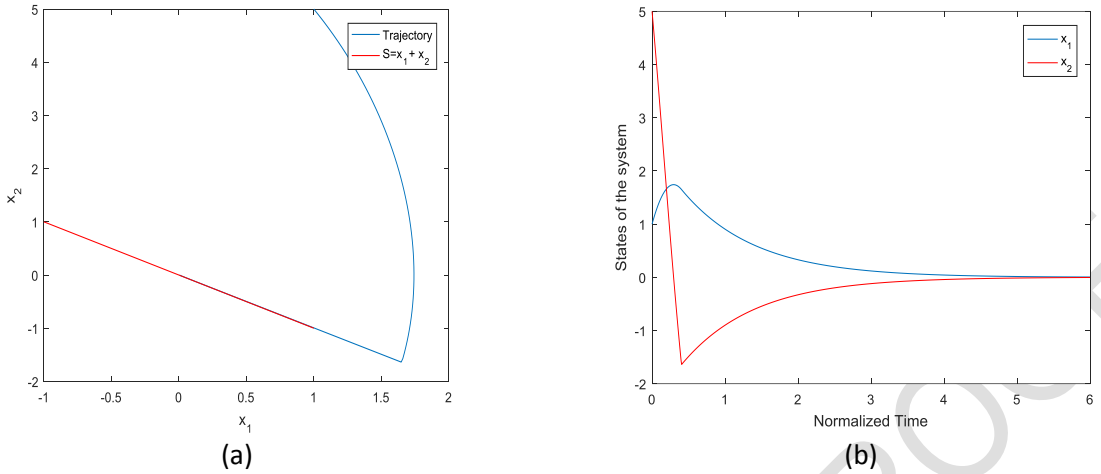

Fig. (2) Vibration suppression using robust adaptive SMC for $x_1(0) = 1, x_2(0) = 5$: (a) the trajectory in the phase plane. (b) the states of the system.

Also, the design parameter of the controller is considered as $K = 1$. Figures. 1 to 5 show the results for the stabilization of the nanobeam based on the proposed control technique with different initial conditions. As it is shown in these figures, the proposed robust adaptive controller, which is equipped with the EKF, could appropriately deal with uncertainties and unexpected noises. These results conspicuously confirm that the system reaches the slide surface after a short period of time and then the states of the system reach their desired values using the suggested controller.

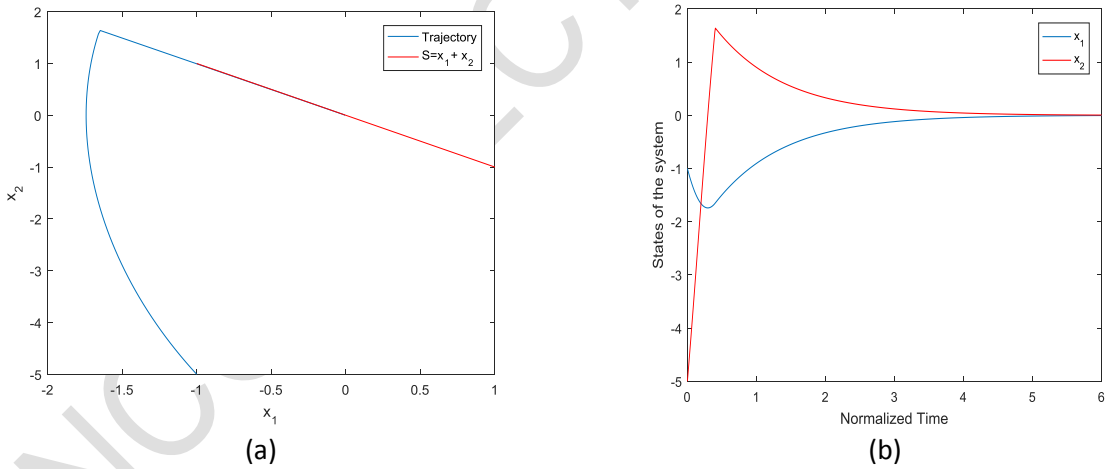

Fig. (3) Vibration suppression using robust adaptive SMC for $x_1(0) = -1, x_2(0) = -5$: (a) the trajectory in the phase plane. (b) the states of the system.

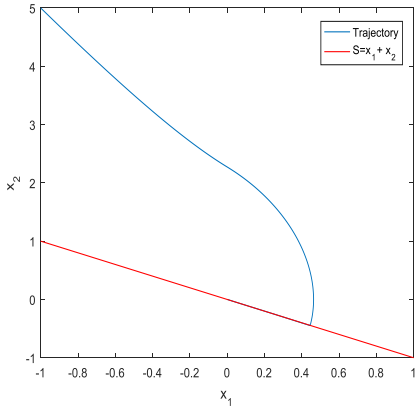

(a)

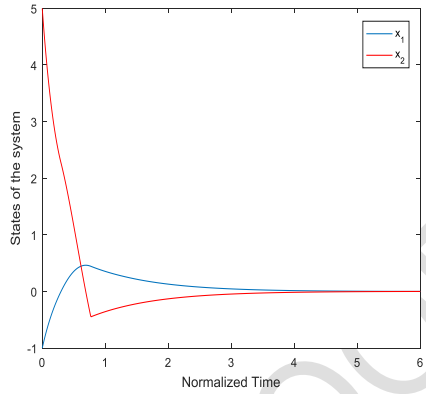

(b)

Fig. (4) Vibration suppression using robust adaptive SMC for $x_1(0) = -1, x_2(0) = 5$:(a) the trajectory in the phase plane. (b) the states of the system.

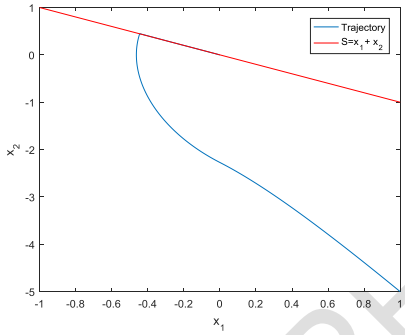

(a)

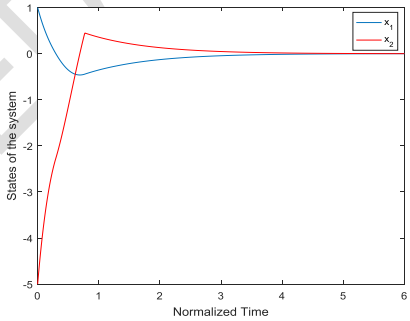

(b)

Fig. (5) Vibration suppression using robust adaptive SMC for $x_1(0) = 1, x_2(0) = -5$ (a) the trajectory in the phase plane. (b) the states of the system.

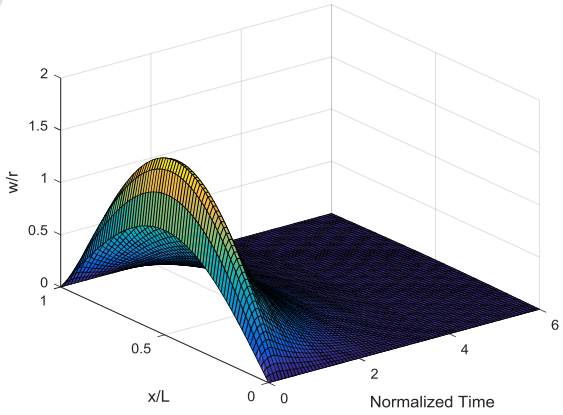

Fig. (6) Time history of deflection of the nanobeam using the proposed controller.

Figure 6 shows the time history of the deflection of the nanobeam using the proposed control scheme, where the nanobeam is completely stabilized after 6 time units. In Figure 7, the performance of the controller for stabilizing the system is depicted for $x_1(0)=5, x_2(0)=15$. In this figure, the estimated states of the system are shown as well. To verify the benefits of the proposed control technique, its performance is compared with a PID controller with $k_p=10$, $k_i=0.1$, and $k_d=15$. Figures 8 and 9 show the results of the stabilization of the nanobeam using the proposed control technique and the PID controller, which verifies the effectiveness of the proposed robust adaptive controller. In summary, the numerical simulations vividly illustrate the performance of the proposed control scheme in different initial conditions for stabilization of the nanobeam when there exist unexpected noises and uncertainties.

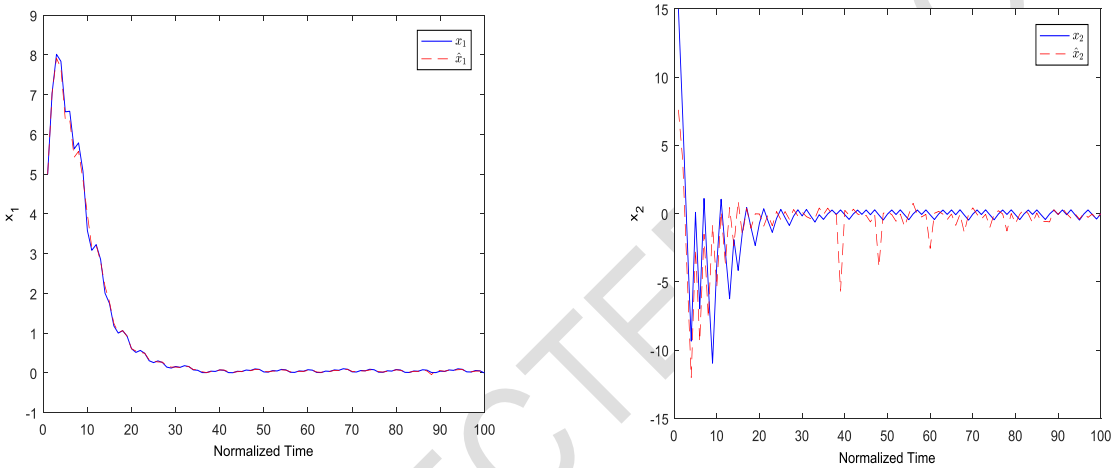

(a) (b)

Fig. (7) Time history of states of the system and the estimated states.

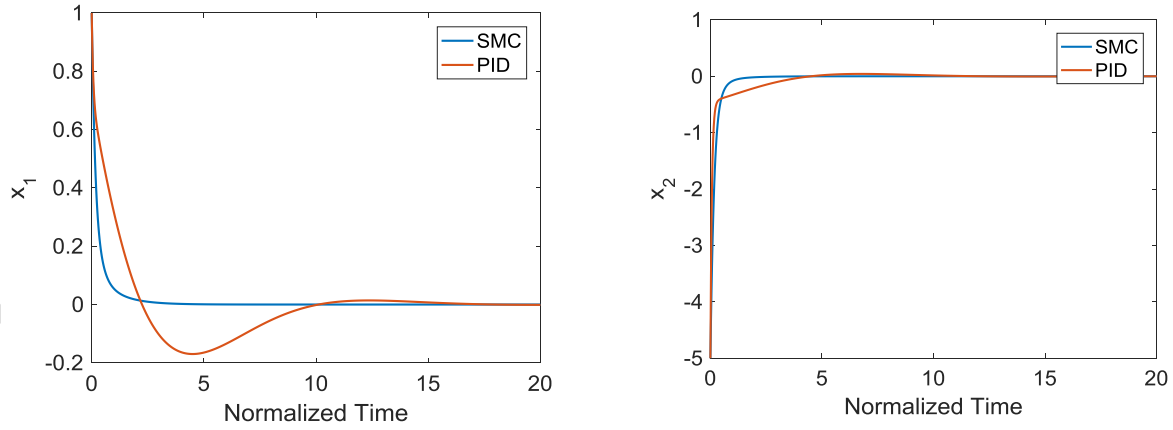

(a) (b)

Fig. (8) Time history of states of the system using SMC and PID.

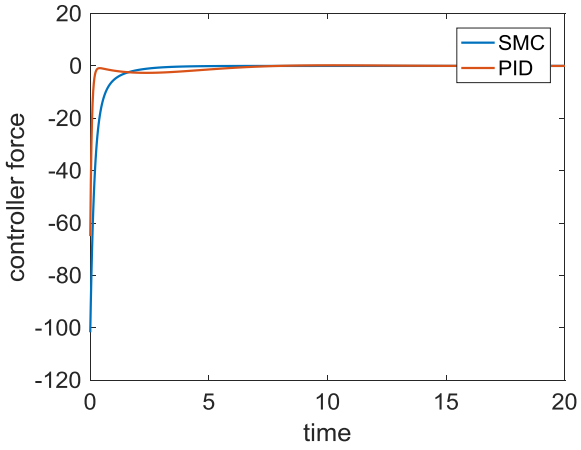

Fig. (9) Control input using SMC and PID.

5. Conclusion

Using Hamilton's principle and the Galerkin approach, a nonlinear ordinary differential equation was derived to study the vibration control of nonlocal strain gradient nanobeams. The robust adaptive SMC was designed to suppress the nonlinear vibration of the nanobeam, which was equipped with the EKF to make it robust against uncertainties and noises due to the lack of accurate information as well as unexpected noises which are prevalent cases in micro/nano-structures. The proof of the stability of the closed-loop system was conducted through the Lyapunov stability theory. Moreover, to illustrate the performance of the suggested control scheme, the numerical simulation results were presented for various initial states. To provide an insight for future work analysis, a data-based vibration analysis is developed for the micro/nanobeams using the neural network [30-34]. Furthermore, using [35-37], a finite-time learning approach is proposed to develop a data-based vibration control for the micro/nanobeams. Finally, using [38, 39], a data-based optimal vibration control is proposed for the micro/nanobeams.

References:

[1] C. Chircov, A.M. Grumezescu, Microelectromechanical systems (mems) for biomedical applications, Micromachines, 13 (2022) 164.

[2] A. Vahidi-Moghaddam, A. Rajaei, R. Vatankhah, M.R. Hairi-Yazdi, Terminal sliding mode control with non-symmetric input saturation for vibration suppression of electrostatically actuated nanobeams in the presence of Casimir force, Applied Mathematical Modelling, 60 (2018) 416-434.

[3] I.V. Uvarov, M.O. Izyumov, Reliability issues for electrostatically actuated MEMS switch, in: International Conference on Micro-and Nano-Electronics 2021, SPIE, 2022, pp. 144-149.

[4] A. Yousefpour, A. Vahidi-Moghaddam, A. Rajaei, M. Ayati, Stabilization of nonlinear vibrations of carbon nanotubes using observer-based terminal sliding mode control, Transactions of the Institute of Measurement and Control, 42 (2020) 1047-1058.

[5] A. Vahidi-Moghaddam, A. Rajaei, R. Vatankhah, M.R. Hairi-Yazdi, Analytical solution for nonlinear vibration of a new arch micro resonator model, Journal of Physics D: Applied Physics, 53 (2020) 285503.

[6] A. Ghaderi, E. Ghavanloo, S. Fazelzadeh, Reliability analysis of carbon nanotube-based nano-truss under various loading conditions, Iranian Journal of Science and Technology, Transactions of Mechanical Engineering, 45 (2021) 1123-1131.

[7] V.A. Aksyuk, F. Pardo, C.A. Bolle, S. Arney, C.R. Giles, D.J. Bishop, Lucent Microstar micromirror array technology for large optical crossconnects, in: MOEMS and Miniaturized Systems, SPIE, 2000, pp. 320-324.

[8] H.-M. Cheng, M.T. Ewe, G.T. Chiu, R. Bashir, Modeling and control of piezoelectric cantilever beam micro-mirror and micro-laser arrays to reduce image banding in electrophotographic processes, Journal of Micromechanics and Microengineering, 11 (2001) 487.

[9] A. Vahidi-Moghaddam, M.R. Hairi-Yazdi, R. Vatankhah, Analytical solution for nonlinear forced vibrations of functionally graded micro resonators, Mechanics Based Design of Structures and Machines, 51 (2023) 1543-1562.

[10] R. Mindlin, H. Tiersten, Effects of couple-stresses in linear elasticity, in, Columbia Univ New York, 1962.

[11] F. Yang, A. Chong, D.C.C. Lam, P. Tong, Couple stress based strain gradient theory for elasticity, International journal of solids and structures, 39 (2002) 2731-2743.

[12] R.D. Mindlin, Second gradient of strain and surface-tension in linear elasticity, International Journal of Solids and Structures, 1 (1965) 417-438.

[13] N. Fleck, J. Hutchinson, A phenomenological theory for strain gradient effects in plasticity, Journal of the Mechanics and Physics of Solids, 41 (1993) 1825-1857.

[14] D.C. Lam, F. Yang, A. Chong, J. Wang, P. Tong, Experiments and theory in strain gradient elasticity, Journal of the Mechanics and Physics of Solids, 51 (2003) 1477-1508.

[15] A.C. Eringen, Nonlocal polar elastic continua, International journal of engineering science, 10 (1972) 1-16.

[16] E.C. Aifantis, On the role of gradients in the localization of deformation and fracture, International Journal of Engineering Science, 30 (1992) 1279-1299.

[17] C. Lim, G. Zhang, J. Reddy, A higher-order nonlocal elasticity and strain gradient theory and its applications in wave propagation, Journal of the Mechanics and Physics of Solids, 78 (2015) 298-313.

[18] C. Xiao, G. Zhang, Y. Yu, Y. Mo, R. Mohammadi, Nonlinear vibration analysis of the nanobeams subjected to magneto-electro-thermal loading based on a novel HSDT, Waves in Random and Complex Media, (2022) 1-20.

[19] A. Rajaei, A. Vahidi-Moghaddam, M. Eghtesad, D. Necsulescu, E.A. Yazdi, Nonsingular decoupled terminal sliding-mode control for a class of fourth-order under-actuated nonlinear systems with unknown external disturbance, Engineering Research Express, 2 (2020) 035028.

[20] A. Vahidi-Moghaddam, A. Rajaei, M. Ayati, R. Vatankhah, M.R. Hairi-Yazdi, Adaptive prescribed-time disturbance observer using nonsingular terminal sliding mode control: Extended Kalman filter and particle swarm optimization, IET Control Theory & Applications, 14 (2020) 3301-3311.

[21] J.K. Moncy, K. Karuturi, Extended Kalman Filter-based Attitude Estimation using Magnetometer-and Sun Sensor-Aided MEMS Gyros, Communication and Control for Robotic Systems, (2022) 221-235.

[22] S. Wang, A. Yousefpour, A. Yusuf, H. Jahanshahi, R. Alcaraz, S. He, J.M. Munoz-Pacheco, Synchronization of a non-equilibrium four-dimensional chaotic system using a disturbance-observer-based adaptive terminal sliding mode control method, Entropy, 22 (2020) 271.

[23] A. Rajaei, A. Vahidi-Moghaddam, M. Ayati, M. Baghani, Integral sliding mode control for nonlinear damped model of arch microbeams, Microsystem Technologies, 25 (2019) 57-68.

[24] A. Rajaei, A. Vahidi-Moghaddam, A. Chizfahm, M. Sharifi, Control of malaria outbreak using a non-linear robust strategy with adaptive gains, IET Control Theory & Applications, 13 (2019) 2308-2317.

[25] A. Vahidi-Moghaddam, A. Rajaei, M. Ayati, Disturbance-observer-based fuzzy terminal sliding mode control for MIMO uncertain nonlinear systems, Applied Mathematical Modelling, 70 (2019) 109-127.

[26] B. Wang, M. Derbeli, O. Barambones, A. Yousefpour, H. Jahanshahi, S. Bekiros, A.A. Aly, M.M. Alharthi, Experimental validation of disturbance observer-based adaptive terminal sliding mode control subject to control input limitations for SISO and MIMO systems, European Journal of Control, 63 (2022) 151-163.

[27] M. Ayati, H. Khaloozadeh, A stable adaptive synchronization scheme for uncertain chaotic systems via observer, Chaos, Solitons & Fractals, 42 (2009) 2473-2483.

[28] R. Vatankhah, F. Karami, H. Salarieh, Observer-based vibration control of non-classical microcantilevers using extended Kalman filters, Applied Mathematical Modelling, 39 (2015) 5986-5996.

[29] J.F. Rhoads, S.W. Shaw, K.L. Turner, The nonlinear response of resonant microbeam systems with purely-parametric electrostatic actuation, Journal of Micromechanics and Microengineering, 16 (2006) 890.

[30] P. Tooranjipour, R. Vatankhah, M.M. Arefi, Prescribed performance adaptive fuzzy dynamic surface control of nonaffine time-varying delayed systems with unknown control directions and dead-zone input, International Journal of Adaptive Control and Signal Processing, 33 (2019) 1134-1156.

[31] P. Tooranjipour, R. Vatankhah, A. Khosravifard, Design of a nonsingular adaptive fuzzy backstepping controller for electrostatically actuated microplates, Applied Mathematical Modelling, 88 (2020) 283-306.

[32] A. Yousefpour, H. Jahanshahi, S. Bekiros, J.M. Muñoz-Pacheco, Robust adaptive control of fractional-order memristive neural networks, in: Mem-Elements for Neuromorphic Circuits with Artificial Intelligence Applications, Elsevier, 2021, pp. 501-515.

[33] A. Yousefpour, H. Jahanshahi, D. Gan, Fuzzy integral sliding mode technique for synchronization of memristive neural networks, in: Mem-Elements for Neuromorphic Circuits with Artificial Intelligence Applications, Elsevier, 2021, pp. 485-500.

[34] P. Tooranjipour, R. Vatankhah, Adaptive critic-based quaternion neuro-fuzzy controller design with application to chaos control, Applied Soft Computing, 70 (2018) 622-632.

[35] A. Vahidi-Moghaddam, M. Mazouchi, H. Modares, Memory-augmented system identification with finite-time convergence, IEEE Control Systems Letters, 5 (2020) 571-576.

[36] A. Vahidi-Moghaddam, M. Mazouchi, H. Modares, Learning dynamics system models with prescribed-performance guarantees using experience-replay, in: 2021 American Control Conference (ACC), IEEE, 2021, pp. 1941-1946.

[37] Z. Li, A. Vahidi-Moghaddam, H. Modares, J. Sun, Adaptive finite-time disturbance rejection for nonlinear systems using an experience-replay based disturbance observer, arXiv preprint arXiv:2007.14565, (2020).

[38] M.R. Hajidavalloo, F.A. Shirazi, M.J. Mahjoob, Performance of different optimal charging schemes in a solar charging station using dynamic programming, Optimal Control Applications and Methods, 41 (2020) 1568-1583.

[39] M.R. Hajidavalloo, F. Ayatolah Zadeh Shirazi, M. Mahjoob, Energy cost minimization in an electric vehicle solar charging station via dynamic programming, Journal of Computational Applied Mechanics, 51 (2020) 275-280.